Insight into hypertrophied hearts: a cardiovascular magnetic resonance study of papillary muscle mass and T1 mapping

Rebecca Kozor[1,2], Sabrina Nordin[1,3], Thomas A Treibel[1,3], Stefania Rosmini[1], Silvia Castelletti[1], Marianna Fontana[4], Gabriella Captur[1], Shanat Baig[5], Richard P. Steeds[5], Derralynn Hughes[6], Charlotte Manisty[1,4], Stuart M Grieve[2], Gemma A Figtree[2], James C Moon[1,3]

1. Barts Heart Centre, London, UK
2. Sydney Medical School, University of Sydney, Australia
3. Institute of Cardiovascular Science, University College London, UK
4. National Amyloidosis Centre, Royal Free Hospital, University College London, UK
5. University Hospitals Birmingham, UK
6. Lysosomal Storage Disorders Unit, Royal Free Hospital, University College London, UK

Short title: Papillary muscle hypertrophy

Corresponding Author:

Dr Rebecca Kozor

Barts Heart Centre, London

Sydney Medical School, The University of Sydney

T: +61 94112649

F: +61 94133329

E: rebeccakozor@gmail.com

Left ventricular hypertrophy (LVH) is common and contributes significantly to cardiovascular risk (1). Its aetiology may be difficult to determine and non-invasive imaging forms an increasingly important part of investigations. LVH can be a physiological adaptation to afterload (eg aortic stenosis (AS), hypertension, athleticism), or may develop as a consequence of an underlying cardiomyopathy (hypertrophic cardiomyopathy, HCM), or infiltration (eg amyloidosis or Fabry disease, FD).

A potential imaging biomarker is the left ventricular papillary muscles (LVPM). These contribute up to 8% of total left ventricular mass (LVM) in the normal heart depending upon analysis technique (2-4). The relationship between LVPM and compacted myocardial hypertrophy appears to be non-linear. In FD, a rare X-linked lysosomal storage disorder resulting in sphingolipid deposition, where there is established LVH, they appear disproportionately hypertrophied, (up to 20% of total LVM) (5, 6). LVPM contribution to total LVM is unknown in other heart conditions and early FD. A wider understanding of the relationship between LVPM hypertrophy and wall hypertrophy is lacking.

Cardiovascular magnetic resonance (CMR) is the 'gold standard' non-invasive method for measuring LVM (5). It is increasingly utilised to differentiate the underlying cause of LVH using myocardial tissue characterisation such as late gadolinium enhancement (LGE) and parametric mapping (T1, T2, T2*). Native T1 mapping aids in the detection of heart muscle pathology by directly measuring a fundamental relaxation property, the longitudinal relaxation time or "T1". This may alter with changes in tissue structural or chemical composition. In general, high septal T1 values can occur with inflammation, oedema, fibrosis and amyloid deposition, and low T1 values can occur with iron deposition and in FD. A low T1 value in FD likely represents sphingolipid accumulation (7). Indeed 85%+ of FD patients with LVH have a low T1, and low T1 values may also precede hypertrophy (8), suggesting storage can be early.

We hypothesised that the LVPM contribution to LVM would be significantly different

between various cohorts of hypertrophied hearts – thereby providing a CMR imaging biomarker to help differentiate between causes of LVH.

Firstly, we aimed to quantify LVPM hypertrophy across a range of heart diseases a) with hypertrophy (LVH+ve) – including afterload (hypertension, AS), cardiomyopathy (HCM) and infiltrations (amyloid and FD), compared to healthy controls, and also b) the same conditions without hypertrophy (LVH-ve) but with proven early or preclinical disease. Secondarily, we sought insights into the biology of LVPM hypertrophy in FD using native T1 mapping.

Methods

Subject populations

Subjects were collected from a single UK centre from six different research CMR cohorts. If previously published or part published, the cohorts have their reference cited. Existing ethics approval was present for all, and all subjects had given written informed consent for their imaging data to be used for research. Both subjects with and without LVH were used in each group (except healthy volunteers). LVH was defined as increased indexed LVM on CMR according to age and gender matched normal reference ranges (9). LVH-ve cases were those with early disease or preclinical disease (eg. gene positive but classic phenotype negative). Inclusion criteria for each cohort were as follows:

1. FD – n=125 comprised of 63 subjects from two previously published cohorts (7, 8) plus 62 prospectively recruited patients as part of an ongoing study; all gene-positive; both males and females; 64 LVH+ve, 61 LVH-ve.
2. HCM – n=85 randomly selected gene-positive patients with LVH, (subjects with isolated apical hypertrophy excluded); 50 LVH+ve plus 35 LVH-ve gene-positive cases from a previously published cohort (10).
3. Cardiac Amyloidosis – n=67 comprised of 50 randomly selected LVH+ve clinical cases (AL and ATTR); 17 LVH-ve LGE positive cases (all AL) from a previously

published cohort (11).

4. AS – n=82 with symptomatic severe AS prior to aortic valve replacement (72 LVH+ve, 10 LVH-ve) as part of an ongoing study.
5. Hypertension – n=40 from a previously published cohort of individuals with documented hypertension recruited from a specialist tertiary centre (14 LVH+ve, 26 LVH-ve) (12).
6. Healthy controls – n=79 all volunteers, all had no history of cardiovascular disease (normal health questionnaire, normal electrocardiogram, no cardioactive medication except for primary prevention). All CMR scans were normal without evidence of LVH.

CMR imaging and analysis

CMRs were acquired using a 1.5 Tesla Avanto (Siemens Healthcare, Erlangen, Germany). Cardiac chamber volumes, LVM and LVPM mass were quantified on all subjects from a pre-contrast breath-held short axis (SAX) stack of balanced steady-state free precession cine images, using CVI42 (Circle Cardiovascular Imaging Inc., Calgary, Canada) and previously described manual contouring methodologies (5) (Example methodology – Figure 1).

T1 mapping data was only analysed for the FD cases and healthy controls. T1 mapping was performed pre-contrast administration on a basal and mid left ventricular SAX slice in diastole using a shortened modified Look-Locker inversion recovery (ShMOLLI) sequence (13). The resulting pixel by-pixel T1 color maps were displayed using a customized 12-bit lookup table, where normal myocardium was green (T1~960ms), increasing T1 was red (T1>1020ms), and decreasing T1 was blue (T1<900ms). For the septal T1 measurement, a region of interest (ROI) in the mid septum was manually drawn, taking care to clearly avoid the blood-myocardial boundary with a 20% offset. LVPM T1 was measured by manually drawing a ROI in the larger of the 2 papillary muscles in the mid-ventricular short axis slice,

again with an offset from the blood-myocardial boundary. Thus, the shape and size of the ROIs in the LVPMs were all different due to the varying size and morphology of the LVPMs. To minimize potential partial volume contamination from the blood pool, only papillary muscles greater than 6mm in diameter were analyzed. This size was chosen to enable a large enough ROI (>0.2cm^2) for pixel analysis. Since T1 is known to vary between field strength, acquisition technique and site, and gender (females typically have higher T1 than males) (14), the normal ranges of T1 values in this study were defined as mean ± 2 standard deviations of the healthy control group in males and females ("low" < 2 SD below the mean; "high" > 2 SD above the mean).

To verify the reproducibility and reliability of measuring papillary muscle T1, the intra- and inter-observer repeatability were assessed in half of the FD subjects. For intra-observer variability, the measurements were performed twice by the same observer (RK) with at least 1 month between measurements. For inter-observer variability, the first observer (RK) measurement was compared to a second independent observer (SN), blinded to initial results.

Late gadolinium enhancement (LGE) imaging was only analysed on the FD cases. These were acquired in a SAX stack and standard long-axis views, plus cross-cuts if LGE+ve, using a FLASH (fast low angle shot) sequence with PSIR, a minimum of 5 minutes after contrast administration (0.1 mmol/kg body weight, Gadoterate meglumine, Dotarem, Guerbet S.A., France).

Statistical analysis

Statistical analyses were carried out using SPSS V22.0 (IBM, Armonk, NY). All continuous variables are expressed as mean ± standard deviation. Categorical variables are expressed as percentages. Subgroup results were compared by either a 2-tailed t-test or 1-way analysis of variance (ANOVA) with post hoc analysis using the Games-Howell procedure (differing variances) or Bonferroni correction if not. A p-value of <0.05 was considered significant. The

Bland Altman test assessed intra- and inter-observer variability of LVPM T1, with the results presented graphically including mean differences, 95% limits of agreement, and the coefficient of repeatability.

Results

There were 478 cases in total: 125 FD (64 LVH+ve, 61 LVH-ve), 85 HCM (50 LVH+ve, 35 LVH-ve), 82 AS (72 LVH+ve, 10 LVH-ve), 67 amyloid (50 LVH+ve – 25 AL, 25 ATTR; 17 LVH-ve, all AL), 40 hypertension (14 LVH+ve, 26 LVH-ve), and 79 healthy controls (all no LVH), Table 1.

LVPM contribution to myocardial mass

LVH+ve cases (n=250): The LVPM contribution to total LVM was not the same in all diseases. FD (13%±3) was significantly more than all other diseases (average 7%; $p<0.001$ for each comparison). HCM (10%±3) was higher than all other diseases except FD ($p<0.001$ for each comparison). All other diseases and controls were similar with LVPMs comprising 7-8% of total LVM, Table 1 (top) and Figure 2.

LVH-ve cases (n=149): The LVPM contribution to total LVM was the same in all conditions and controls (mean 7%) except FD, which was higher than all other diseases and controls (11%±3; $p<0.001$ for each comparison), Table 1 (bottom) and Figure 3.

T1 measurements of papillary muscles

The T1 of LVPMs was measured in FD and controls. Septal T1 was measured in all, but LVPM T1 could only be measured in LVPMs >6mm, so 111 (89%) FD and 73 controls (92%) were analysed (Table 2, Figure 4).

Controls (n=73): The mean septal T1 was 958±28 ms (902ms lower limit, LL), with males 947±23ms (LL 901ms) and females 972±28ms (LL 916ms). The mean LVPM T1 was 970±37ms, with the LL in males 915ms and females 926ms. The LVPM contribution to LVM was the same in males and females (7±1%).

LVH+ve FD cases (n=59): 92% had low septal T1 (8% normal). LVPM T1 was substantially concordant with septal T1: When the septal T1 was low, the LVPM T1 was low in 90% (49/54), and when the septal T1 was normal, the LVPM T1 was normal in 40% (2/5). Between the low and normal septal T1 groups, the LVPM contribution to LVM was similar (12±3% vs 14±2%, p=0.4).

Gadolinium was administered to 78% (n=87) of the FD group, with 55% of these demonstrating LGE – 24 males (all LVH+ve) and 23 females (15 LVH+ve). Of the LVH+ve group, 48 received gadolinium – 35/44 were LGE+ve with low septal T1, and 4/4 were LGE+ve with normal septal T1. All LVH+ve FD cases with normal septal T1 had LGE in their LV myocardium (Table 2, last panel).

LVH-ve FD cases (n=52): 54% had low septal T1 (46% normal). There was less concordance than in the LVH+ve group: When the septal T1 was normal, the LVPM T1 was normal in 70% (17/24), and when the septal T1 was low, 75% (21/28) had a concordant low LVPM T1. Despite these findings, LVPM contribution to LVM was similar between the low septal T1 and normal septal T1 groups (11±3% vs 10±3%, p=0.08). Of this LVH-ve group, 39 received gadolinium – 5/18 were LGE+ve with low septal T1, and 3/21 were LGE+ve with normal septal T1.

The same pattern of results was seen when dividing these FD subgroups into males and females (Supplementary Table 1). All FD subjects had good LV systolic function (LVEF

75±7%), and 64% (n=71) were treated with enzyme replacement therapy (ERT). There was no statistical difference in LVPM contribution to LVM in those FD patients treated with ERT compared to those FD patients not receiving ERT (12±4% vs 11±3%, p=0.2). In addition, T1 values were non-significantly lower in FD patients on ERT compared to FD patients not on ERT: septal T1 872±58ms vs 898±48ms, p=0.08, and LVPM T1 890±63ms vs 907±51ms, p=0.3.

Intra- and inter-observer variability

Assessment of the intra- and inter-observer variability by Bland Altman plots and coefficients of repeatability showed acceptable levels of agreement for measurements of LVPM T1 (Figure 5).

Discussion

Subjects with FD had disproportionately high LVPM hypertrophy compared to all the LVH+ve cohorts and healthy controls. HCM also had significantly increased LVPM contribution to total LVM compared to all other LVH+ve groups except for FD. Interestingly, it was only FD that displayed LVPM hypertrophy in FD in the absence of LVH, contributing over 1.5 times as much of the proportion of total mean LVM compared to controls. These findings support the hypothesis that the LVPMs are an imaging biomarker helpful in differentiating the aetiology of LVH, and may even be useful in LVH-ve hearts. It is acknowledged that the LVPMs are small structures and the absolute observed differences in LVPM quantification are small, despite being statistically significant. This disputes the robustness for clinical application. Furthermore, the level of image resolution and contrast required to precisely measure LVPM mass can only be achieved with CMR, which already allows further differentiation of aetiologies with tissue characterisation.

The T1 mapping findings offer further insight into the biology of cardiac involvement in FD.

This was especially interesting in the LVH-ve FD cases with concordant normal septal and LVPM T1 values (indicating no detectable storage) but disproportionate LVPM hypertrophy. This phenomenon of hypertrophy in the absence of detectable storage implies there may be another mechanism for the LVPM hypertrophy other than or in addition to sphingolipid deposition (eg. toxic metabolites, oedema, inflammation). However, this is difficult to ascertain because of the limitations of using this technique on such small structures. One such potential limitation of using LVPM T1 as a surrogate marker of sphingolipid accumulation in FD is that pixels of interest in the LVPMs may be subject to partial volume effects from the adjacent blood pool, given they are small structures within the ventricular cavity. This partial volume effect might result in LVPM 'pseudonormalisation' whereby the true native LVPM T1 may be lower than reported. Future research will enable investigation into whether LVPM T1 is lower than the septum, or reduced prior to septal T1 lowering, indicating preferential sphingolipid deposition in the LVPMs – a potential pathophysiological explanation of their exaggerated hypertrophy. Alternatively, a normal LVPM T1 may be pseudonormalisation from concurrent scar, or as a consequence of ERT. Histological confirmation would be helpful in dissecting this issue, but unfortunately was not available.

Another limitation is of the reliability of T1 mapping in detecting storage. Future research into the native multi parametric signal of myocardium might reveal whether a 'normal' T1 value truly represents no sphingolipid storage. There may be a detection threshold – a certain storage burden may need to be reached to permit a measurable drop in T1. We acknowledge that histological validation is essential in exploring this issue, but myocardial tissue is difficult to obtain in this disease so was not pursued. Also, correlation of LVPM CMR findings to patient outcomes or symptomatology was beyond the scope of this work.

This study also highlights that the paradigm of disease progression in FD is not well understood, and that the relationship between myocardial hypertrophy, scar and storage in the heart is yet to be unravelled. A large ongoing multicentre study in FD using CMR is currently

being undertaken to further investigate the biology of cardiac involvement in FD.

In summary, the papillary muscles may be useful in differentiating the underlying cause of LVH, although clinical overlap does exist. They are also useful in LVH-ve hearts, where disproportionate LVPM hypertrophy is seen in FD. Low T1 is not associated with additional LVPM hypertrophy implicating other pathological mechanisms involved in LVPM hypertrophy in FD.

Acknowledgments: none

Disclosures:

RK was sponsored by a Heart Research Australia Grant funded by Shire.

References

1. Gupta S, Berry JD, Ayers CR, Peshock RM, Khera A, de Lemos JA, et al. Left ventricular hypertrophy, aortic wall thickness, and lifetime predicted risk of cardiovascular disease:the Dallas Heart Study. JACC Cardiovascular imaging. 2010;3(6):605-13.

2. Vogel-Claussen J, Finn JP, Gomes AS, Hundley GW, Jerosch-Herold M, Pearson G, et al. Left ventricular papillary muscle mass: relationship to left ventricular mass and volumes by magnetic resonance imaging. Journal of computer assisted tomography. 2006;30(3):426-32.

3. Papavassiliu T, Kuhl HP, Schroder M, Suselbeck T, Bondarenko O, Bohm CK, et al. Effect of endocardial trabeculae on left ventricular measurements and measurement reproducibility at cardiovascular MR imaging. Radiology. 2005;236(1):57-64.

4. Chuang ML, Gona P, Hautvast GL, Salton CJ, Blease SJ, Yeon SB, et al. Correlation of trabeculae and papillary muscles with clinical and cardiac characteristics and impact on CMR measures of LV anatomy and function. JACC Cardiovascular imaging. 2012;5(11):1115-23.

5. Kozor R, Callaghan F, Tchan M, Hamilton-Craig C, Figtree GA, Grieve SM. A disproportionate contribution of papillary muscles and trabeculations to total left ventricular mass makes choice of cardiovascular magnetic resonance analysis technique critical in Fabry disease. Journal of cardiovascular magnetic resonance. 2015;17:22.

6. Niemann M, Liu D, Hu K, Herrmann S, Breunig F, Strotmann J, et al. Prominent papillary muscles in Fabry disease: a diagnostic marker? Ultrasound in medicine & biology. 2011;37(1):37-43.

7. Sado DM, White SK, Piechnik SK, Banypersad SM, Treibel T, Captur G, et al. Identification and assessment of Anderson-Fabry disease by cardiovascular magnetic resonance noncontrast myocardial T1 mapping. Circulation Cardiovascular imaging. 2013;6(3):392-8.

8. Pica S, Sado DM, Maestrini V, Fontana M, White SK, Treibel T, et al. Reproducibility of native myocardial T1 mapping in the assessment of Fabry disease and its role in early detection of cardiac involvement by cardiovascular magnetic resonance. Journal of cardiovascular magnetic resonance. 2014;16:99.

9. Maceira AM, Prasad SK, Khan M, Pennell DJ. Normalized left ventricular systolic and diastolic function by steady state free precession cardiovascular magnetic resonance. Journal of cardiovascular magnetic resonance. 2006;8(3):417-26.

10. Captur G, Lopes LR, Patel V, Li C, Bassett P, Syrris P, et al. Abnormal cardiac formation in hypertrophic cardiomyopathy: fractal analysis of trabeculae and preclinical gene expression. Circulation Cardiovascular Genetics. 2014;7(3):241-8.

11. Fontana M, Pica S, Reant P, Abdel-Gadir A, Treibel TA, Banypersad SM, et al. Prognostic Value of Late Gadolinium Enhancement Cardiovascular Magnetic Resonance in Cardiac Amyloidosis. Circulation. 2015;132(16):1570-9.

12. Treibel TA, Zemrak F, Sado DM, Banypersad SM, White SK, Maestrini V, et al. Extracellular volume quantification in isolated hypertension - changes at the detectable limits? Journal of cardiovascular magnetic resonance. 2015;17(1):74.

13. Piechnik SK, Ferreira VM, Dall'Armellina E, Cochlin LE, Greiser A, Neubauer S, et al. Shortened Modified Look-Locker Inversion recovery (ShMOLLI) for clinical myocardial T1-mapping at 1.5 and 3 T within a 9 heartbeat breathhold. Journal of cardiovascular magnetic resonance. 2010;12:69.

14. Piechnik SK, Ferreira VM, Lewandowski AJ, Ntusi NA, Banerjee R, Holloway C, et al. Normal variation of magnetic resonance T1 relaxation times in the human population at 1.5 T using ShMOLLI. Journal of cardiovascular magnetic resonance. 2013;15:13.

Table 1. Characteristics of the LVH+ve and LVH-ve cohorts plus controls

	Age (yrs)	Males (%)	LVEDV (ml)	LVEF (%)	LVM (g)	LVPM (%)
LVH+ve cases						
Fabry (n=64)	52 ± 11	64	136 ± 34	76 ± 7	219 ± 75	13 ± 3*γ
HCM (n=50)	51 ± 15	56	129 ± 26	78 ± 7	187 ± 72	10 ± 3*
Amyloid (n=50)	68 ± 11	78	126 ± 30	59 ± 15	209 ± 71	8 ± 2
AS (n=72)	70 ± 11	79	132 ± 26	69 ± 12	194 ± 33	7 ± 3
Hypertension (n=14)	49 ± 16	64	151 ± 45	68 ± 11	190 ± 59	7 ± 2
Controls (n=79)	49 ± 14	56	132 ± 27	71 ± 6	105 ± 26	7 ± 1
LVH-ve cases						
Fabry (n=61)	39 ± 14	18	126 ± 23	74 ± 7	109 ± 23	11 ± 3*γ
HCM (n=35)	31 ± 14	31	124 ± 25	73 ± 6	98 ± 23	7 ± 2
Amyloid (n=17)	58 ± 14	29	117 ± 22	67 ± 11	124 ± 29	7 ± 2
AS (n=10)	70 ± 9	10	103 ± 21	79 ± 7	96 ± 15	7 ± 1
Hypertension (n=26)	61 ± 12	42	124 ± 23	71 ± 8	111 ± 22	7 ± 1

* = $p<0.001$ compared to controls, γ = $p<0.001$ compared to HCM

LVH= left ventricular hypertrophy; HCM= hypertrophic cardiomyopathy; AS= aortic stenosis

Table 2. LVPM contribution to total LVM and T1 values in the FD cohort stratified by LVH, plus healthy controls. Also shows cases with LGE in LV myocardium.

	LVPM (%)	LVPM T1 (ms)	Septal T1 (ms)	LGE+ve
Fabry LVH+ve (n=59)				
Low septal T1 (n=54)	12 ± 3	856 ± 49	846 ± 41	35/44
Normal septal T1 (n=5)	14 ± 2	921 ± 43	930 ± 18	4/4
Fabry LVH-ve (n=52)				
Low septal T1 (n=28)	11 ± 3	898 ± 36	877 ± 29	5/18
Normal septal T1 (n=24)	10 ± 3	939 ± 45	947 ± 28	3/21
Controls (n=73)	7 ± 1	970 ± 37	958 ± 28	-

Note: only FD patients with both septal and LVPM T1 values were included in these analyses (n=111), and LGE imaging in n=87.

LVPM= left ventricular papillary muscles; LVM= left ventricular mass; FD= Fabry disease; LVH= left ventricular hypertrophy

Supplementary Table 1. LVPM contribution to total LVM and T1 values in male and female FD cohorts plus male and female controls

Males Only	LVPM (%)	LVPM T1 (ms)	Septal T1 (ms)
Fabry LVH+ve (n=37)			
Low septal T1 (n=37)	12 ± 3	839 ± 39	831 ± 37
Normal septal T1 (n=0)	-	-	-
Fabry LVH-ve (n=9)			
Low septal T1 (n=5)	12 ± 3	869 ± 43	851 ± 25
Normal septal T1 (n=4)	9 ± 3	932 ± 48	933 ± 22
Male controls (n=44)	7 ± 1	961 ± 30	947 ± 23
Females Only			
Fabry LVH+ve (n=22)			
Low septal T1 (n=17)	13 ± 3	893 ± 42	879 ± 27
Normal septal T1 (n=5)	14 ± 2	921 ± 43	930 ± 18
Fabry LVH-ve (n=43)			
Low septal T1 (n=23)	11 ± 3	904 ± 30	882 ± 27
Normal septal T1 (n=20)	10 ± 3	941 ± 45	950 ± 28
Female controls (n=29)	7 ± 1	982 ± 42	972 ± 28

Note: only FD patients with both septal and LVPM T1 values were included in these analyses (total n=111)

LVPM= left ventricular papillary muscles; LVM= left ventricular mass; FD= Fabry disease; LVH= left ventricular hypertrophy

Figure 1. Representative contour tracings in mid-ventricular short-axis cine slices depicting end-diastolic epicardial (green), endocardial (red) and LVPM (pink) borders in LVH+ve (A) FD, (B) HCM, (C) amyloid, (D) AS, (E) hypertension, and (F) healthy control (no LVH)

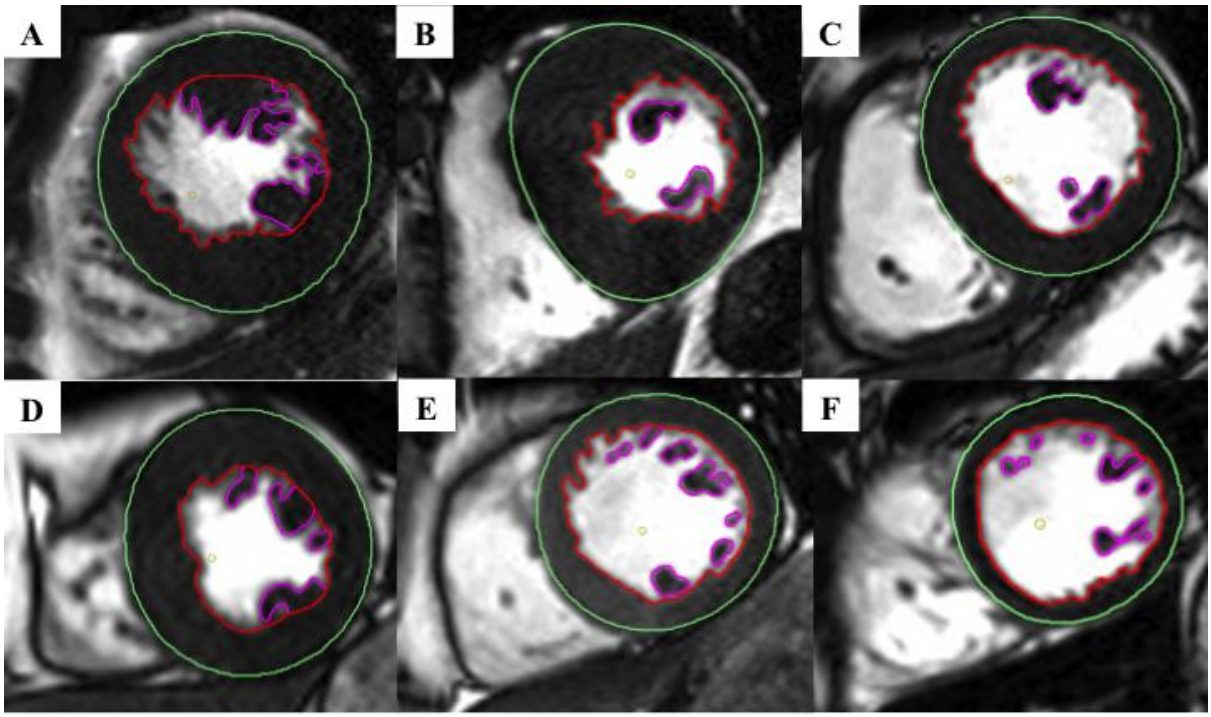

LVH= left ventricular hypertrophy; FD= Fabry disease, HCM= hypertrophic cardiomyopathy; AS= aortic stenosis

Figure 2. Box plots showing LVPM contribution to total LVM in LVH+ve cohorts

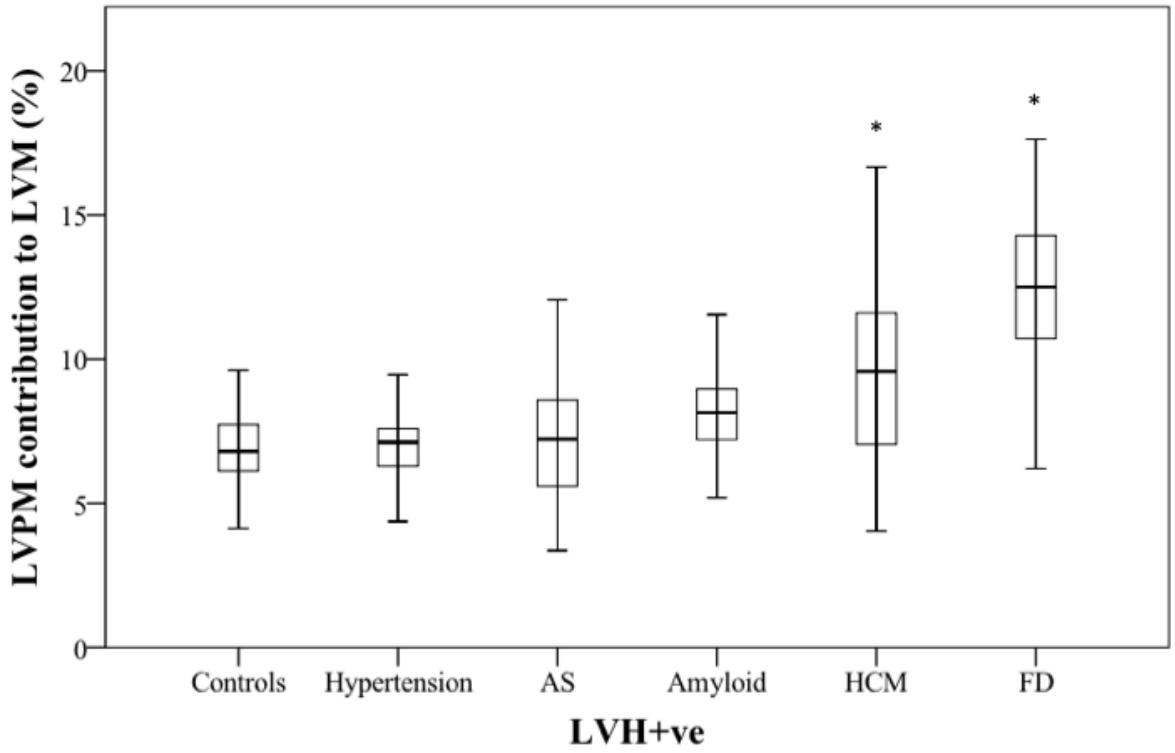

Box plot: box length represents the interquartile range; horizontal box line represents the median; whiskers represent the maximum and minimum values; * denotes $p<0.001$ compared to controls.

LVPM= left ventricular papillary muscles; LVM= left ventricular mass; AS= aortic stenosis; HCM= hypertrophic cardiomyopathy; FD= Fabry disease; LVH+ve= left ventricular hypertrophy positive.

Figure 3. Box plots showing LVPM contribution to total LVM in LVH-ve cohorts

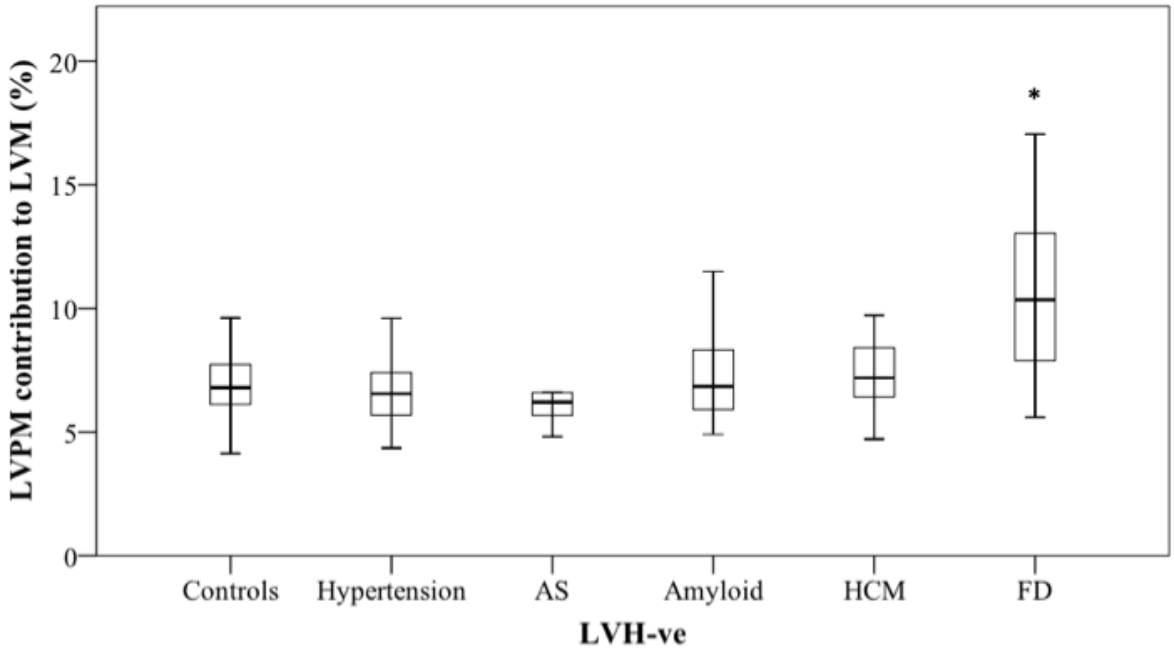

Box plot characteristics as in Figure 2.

LVPM= left ventricular papillary muscles; LVM= left ventricular mass; AS= aortic stenosis; HCM= hypertrophic cardiomyopathy; FD= Fabry disease; LVH-ve= left ventricular hypertrophy negative.

Figure 4. (A) ShMOLLI generated T1 colour map of a representative FD case showing a mid-ventricular short-axis slice with manual contouring and ROIs in the septum and LVPM (green represents normal T1, blue represents low T1). (B) Scatter plot showing the distribution of septal and LVPM T1 values in LVH+ve and LVH-ve FD cases.

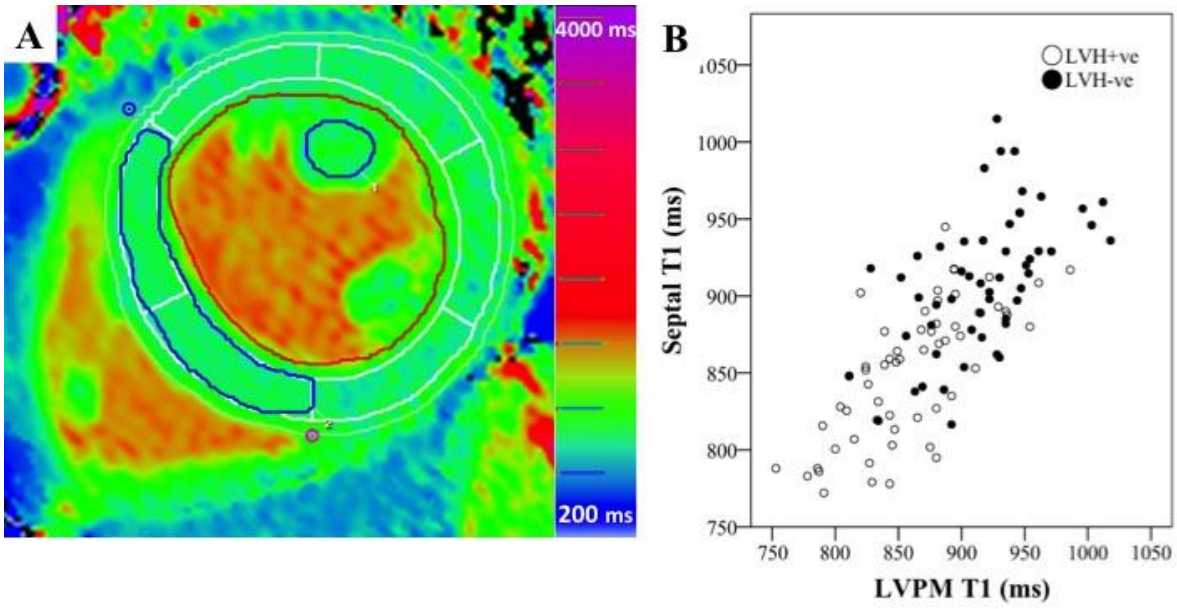

ShMOLLI= shortened modified Look-Locker inversion recovery sequence; FD= Fabry disease; ROI= region of interest; LVPM= left ventricular papillary muscle; LVH= left ventricular hypertrophy

Figure 5. Bland Altman graphs of LVPM analyses of (A) intra-observer variability, and (B) inter-observer variability. The mean difference of each plot is shown as a solid line and the upper and lower limits of agreement as dashed lines. The coefficient of repeatability for each analysis is displayed inset each graph.